ACES Asian Chemical Editorial Society
doi.org/10.1002/asia.202400964
Check for updates
CHEMISTRY
AN ASIAN JOURNAL
Research Article
www.chemasianj.org

Synthesis and Structures of Oxide -Centred Alkali Metal (K, Li)/Lanthanoid (Ln3 or 4) 3,5-Dimethylpyrazolate Cages - Herbert Schumann Revisited

Daniel Werner,[a] Zhifang Guo,[b] Glen B. Deacon,[a] and Peter C. Junk*[b]

Dedicated to Prof. Dr. Inge Schumann in memory of Prof. Dr. Herbert Schumann's pioneering work on lanthanoid pyrazolates and his friendship over many years.

Reaction of lanthanoid tris(3,5-dimethylpyrazolate) compounds, $[Ln(Me_2pz)_3(thf)]_2$ (Ln = La **1a**, Ce, Pr, Dy **1b**, Yb, Lu) with potassium or lithium bistrimethylsilylamide and with or without added 3,5-dimethylpyrazole, or of lanthanoid tris(bistrimethylsilyl)amide complexes with potassium bistrimethylsilylamide and 3,5-dimethylpyrazole have yielded a variety of oxide centred Ln_3 or Ln_4/(K or Li)$_{1-3}$ multinuclear cages, namely, $[La_4O(Me_2pz)_{11}K(thf)_2]$ (**2a**), $[La_4O(Me_2pz)_{11}Li(Me_2pzH)]\cdot0.5$Hexane (**2b**), $[La_4O(Me_2pz)_{10}(Me_2pzH)]$ (**2c**) (from heating **1a** in toluene), $[Ce_3O(Me_2pz)_9K_2(dme)_2]$ (**3a**), $[Ce_3O(Me_2pz)_9Li_2(thf)_2]\cdot0.5$Hexane (**3b**) and $[Ce(Me_2pz)_5Li_2(thf)_3]$ (**3c**), which crystallized together, $[Ce_3O(Me_2pz)_{10}K_3(thf)_3]$ (**3d**), $[Pr_3O(Me_2pz)_{10}K_3(thf)_3]$ (**4**), $[Dy_3O(Me_2pz)_9K_2(thf)_2]\cdot$THF (**5**), $[Yb_3O(Me_2pz)_9K_2(thf)_2]\cdot$THF (**6**), and $[Lu_3O(Me_2pz)_9K_2(thf)_2]\cdot$THF (**7**). Crystals of $\{[K_8(Me_2pz)_8(thf)_2]\cdot THF\}_\infty$ (**8**) were also obtained from the preparation of **7**. From reaction of $[Ce(Me_2pz)_3(thf)]_2$ with potassium *tert*-butoxide in toluene, the cerium(IV) heterobimetallic polymer $[Ce_2(Me_2pz)_6(OtBu)_4K_2]_\infty$ (**9**) was isolated.
In the Ln_3O and the Ln_4O cages, the Ln atoms have triangular and distorted tetrahedral arrangements about the central oxygen, respectively. The relationship of the alkali metals to the central oxygen varies considerably. Thus in **2a**, **2b**, there is no bonding, in **3a**, both K atoms interact weakly, in **3b** one of the two Li atom is bound, in **3d**, **4**, one of three K atoms in bound, whilst in **5–7**, both K atoms are bound. All metals are bound to the cages by a variety of pyrazolate binding modes, with up to five different exhibited in some structures, and a new coordination mode, μ_4-1κ(N):2κ(N′):η^5:η^5, was observed in two complexes. In the structure of **2c**, the coordinated Me_2pzH ligand binds to two metals through a single nitrogen, the first time this has been observed for a pyrazole donor. The complex **9** is polymeric with all metals bridged by butoxide donors as well as by Me_2pz groups.

Introduction

In 1989, Herbert Schumann et al. reported the first structurally characterized lanthanoid pyrazolates with the syntheses of $[Ln_3(\mu\text{-}Me_2pz)_6(\eta^2\text{-}Me_2pz)_3(\mu_3\text{-}O)Na_2(thf)_2]$ (Ln = Y, Ho, Yb, Lu; Me_2pz = 3, 5-dimethylpyrazolate; thf = tetrahydrofuran) and $[Ln_3(\mu\text{-}Me_2pz)_6(\eta^2\text{-}Me_2pz)_3(\mu_3\text{-}O)Na_2(Me_2pzH)_2]$ (Ln = Y, Ho, Yb) by metathesis reactions between sodium 3, 5-dimethylpyrazolate and lanthanoid trihalides in tetrahydrofuran and toluene respectively.[1] The formation of the oxo cages was attributed to the presence of traces of water in the solvents. This suggested the target $Ln(Me_2pz)_3$ complexes were exceptionally sensitive to water, as only 0.015 g was needed in the 200 ml of thf used to achieve the yield of the first group of complexes. This has led to extensive development of lanthanoid pyrazolates, which have contributed notably to the development of new pyrazolate binding models.[2] The extremely high reactivity to water shown by lanthanoid 3,5-dimethylpyrazolates does not appear to extend to other commonly used pyrazolates, such as unsubstituted pyrazolates,[3] 3,5-di-tertbutylpyrazolates[4,5] and 3,5-diphenylpyrazolates,[6] though all need to be handled in an inert atmosphere. Subsequently, a number of $[Ln(Me_2pz)_3(thf)]_2$ complexes have been successfully prepared,[7–9] and structurally characterized,[7–9] and show a change from μ-η^5:η^2 coordination with Ce and Pr to 1κ(N):2κ(N′) coordination and μ-O(thf) bridging from Nd–Lu. Even homoleptic $[Ln(Me_2pz)_3]_n$ and $[Ce(Me_2pz)_3]_4$ have been structurally characterized, the former polymerising through μ-η^5:η^2-Me_2pz groups, and the latter remarkably showing six different pyrazolate binding modes.[10] The Ce^{IV} complex $[Ce(\eta^2\text{-}Me_2pz)_3(\mu\text{-}\eta^2\text{:}\eta^2\text{-}Me_2pz)]_2$ has also been obtained.[11]

Early implications[1] that lanthanoid 3,5-dimethylpyrazolates are associated with high reactivity has been recently exemplified particularly by studies of cerium(III and IV) derivatives. Thus, reaction of $[Ce(Me_2pz)_4]_2$ with 1,4-hydroquinone and of $[Ce(Me_2pz)_3(thf)]_2$ with 1,4-benzoquinone led to the same

---

[a] D. Werner, G. B. Deacon
School of Chemistry, Monash University, Clayton Vic 3800, Australia

[b] Z. Guo, P. C. Junk
College of Science and Engineering, James Cook University,Townsville, Qld 4811, Australia
E-mail: peter.junk@jcu.edu.au

Supporting information for this article is available on the WWW under https://doi.org/10.1002/asia.202400964

intermediate, which undergoes C=O activation.[11] [La-$(Me_2pz)_3(thf)]_2$ caused C=O activation of 1,4-benzoquinone,[11] $[Ce(Me_2pz)_4]_2$ and $[Ln(Me_2pz)_3(thf)]$ (Ln = La, Ce, Lu) undergo reversible benzophenone insertion into Ln-Me_2pz bonds, with Ce^{IV} more reactive than Ln^{III}.[12] Even more striking is the complete but reversible insertion of CO_2 into Ce-Me_2pz bonds of both homoleptic $[Ce(Me_2pz)_4]_2$ and $[Ce(Me_2pz)_3]_4$, and this property has been developed into a catalytic application.[13] Still more recently, we have found that an attempt to prepare $Sc(Me_2pz)_3$ by reaction of Sc metal with $Hg(C_6F_5)_2$ and Me_2pzH in thf in a silicone-greased flask followed by a lengthy crystallization period yielded $[Sc_2(Me_2pz)_4(Me_2pz(SiMe_2O))_2]$, resulting from Me_2SiO insertion into a Sc–N bond of a coordinated pyrazolate.[14] Further, pre-prepared $[Ce(Me_2pz)_3(thf)]_2$ on being heated in toluene in a silicone-greased flask yielded $[Ce_4O(Me_2pz)_9(Me_2pzSiMe_2O)_2]$, a mixed $Ce^{III/IV}$ complex again resulting from Me_2SiO insertion, and the further oxido cage $[Ce_4O(Me_2pz)_{11}]$, the oxido centres being reminiscent of the Schumann cages.[1] Furthermore, the insertion of dimethylsilicone into the Ln–N bond of cyclopentadienyl lanthanoid pyrazolate complexes has been observed.[15]

Heterobimetallic complexes are of particular interest, as not only do they provide access to the properties of both metals, but synergic effects may be observed. In the case of alkali metal/lanthanoid or transition metal bimetallics, their use as reagents in metathesis reactions can deliver main group, transition metal, or lanthanoid heterobimetallics with applications in magnetochemistry, biological systems and photochemistry.[16–17]

We now report the synthesis and structures of a plethora of lanthanoid/alkali metal 3,5-dimethylpyrazolate heterometallic oxide centred cages, mainly containing La/K or Ce/K, but extending to Pr, Dy, Yb and Lu, and to Li in addition to K. These emerged from attempts to prepare $[K_nLn(Me_2pz)_{3+n}](solv)_m$ heterometallics, mainly by reactions of $Ln(Me_2pz)_3$ complexes with Me_2pzH and $K[N(SiMe_3)_2]$, the products again reminiscent of the Schumann cages, but with quite different and more complex structures. Further, when $Ln(Me_2pz)_3$ were treated with $KN(SiMe_3)_2$ without Me_2pzH, to target $[K_nLn(Me_2pz)_3(N(SiMe_3)_2)_n]$ species, cages were also obtained similar to those from reactions in the presence of Me_2pzH. Once cages emerged as products, we were keen to explore the generality of the syntheses, as their appearance has been rare since the original Schumann work. Included is a new pyrazolate binding mode, namely μ_4-1κ(N):2κ(N′):η^5:η^5. Given the plethora of known pyrazolate coordination modes[2,10] the emergence of another is a surprise. In addition, coordination of a pyrazole nitrogen to two different metals was observed for the first time. The products have potential as reagents to prepare other Ln containing oxido bimetallics by metathesis reactions where the alkali metal is replaced.

Results and Discussion

Most syntheses of Ln/K or Li cages except two, used $[Ln(Me_2pz)_3(thf)]_2$ (Ln = La (1a), Ce, Pr, Nd, Dy(1b), Ho, Yb and Lu) complexes as reagents and they were obtained by the reaction of Ln metal, $Hg(C_6F_5)_2$ and Me_2pzH,[7,9] with the application to Ln = Dy being new (Scheme 1). Known structures indicate a structural discontinuity between La–Pr and Nd–Lu.[9] The former are formally 10-coordinate dimers with two terminal η^2-Me_2pz, one terminal thf, one μ-η^5-Me_2pz, and one μ-η^2-Me_2pz binding to each Ln atom, whereas the latter are eight coordinate dimers with two η^2-Me_2pz, two 1κ(N):2κ(N′)-Me_2pz and two bridging thf ligands on each Ln atom. In this study the structure of Ln = La, previously only identified from unit cell, was determined placing it in the first class, whilst that of new complex Ln = Dy was shown to belong to the second (Scheme 1, Figure S1 and S2).

A range of novel lanthanoid-alkali metal oxide cages, $[La_4O(Me_2pz)_{11}K(thf)_2]$ (**2a**), $[La_4O(Me_2pz)_{11}Li(Me_2pzH)]\cdot 0.5Hexane$ (**2b**), $[La_4O(Me_2pz)_{10}(Me_2pzH)]$ (**2c**), $[Ce_3O(Me_2pz)_9K_2(dme)_2]$ (**3a**), $[Ce_3O(Me_2pz)_9Li_2(thf)_2]\cdot 0.5Hexane$ (**3b**), $[Ce(Me_2pz)_5Li_2(thf)_3]$ (**3c**), $[Ce_3O(Me_2pz)_{10}K_3(thf)_3]$ (**3d**), $[Pr_3O(Me_2pz)_{10}K_3(thf)_3]$ (**4**), $[Ln_3O(Me_2pz)_9K_2(thf)_2]\cdot THF$ (Ln = Dy (**5**), Yb (**6**), and Lu (**7**)), containing either Ln_3O or Ln_4O units, have been prepared mainly by reactions of lanthanoid tris(3,5-dimethylpyrazolates) with alkali metal bistrimethylsilylamides with (2a, 2b, 3a Scheme 2 method a), or without (3b, 3c, 4, 5, 7 Scheme 2 method b) additional 3,5-dimethylpyrazole. In two cases, lanthanoid tris(bistrimethylsilylamides) were used together with the alkali metal bistrimethylsilylamide and an appropriate amount of Me_2pzH (3d, 6 Scheme 2 method c). The synthesis of **7** was accompanied by formation of $\{[K_8(Me_2pz)_8(thf)_2]\cdot THF\}_\infty$ (**8**) (Scheme 2 method c). Complex **2c** was obtained by heating $[La(Me_2pz)_3(thf)]_2$ under reflux in toluene (Scheme 2 method d). The stoichiometries employed are shown in Scheme 2. The non-oxido bimetallic **3c**, which is an original target molecule, crystallized with **3b**. Even a reaction between cerium tris(3,5-dimethylpyrazolate) and potassium *tert*-butoxide that did not result in an oxide cage, still involved oxidation as the resulting bimetallic $[Ce_2(Me_2pz)_6(OtBu)_4K_2]_\infty$ (**9**), contains cerium(IV).

The source of oxygen in the cages and the cause of oxidation of cerium(III) to cerium(IV) to give **9** is probably a trace of water or oxygen in agreement with Schumann's

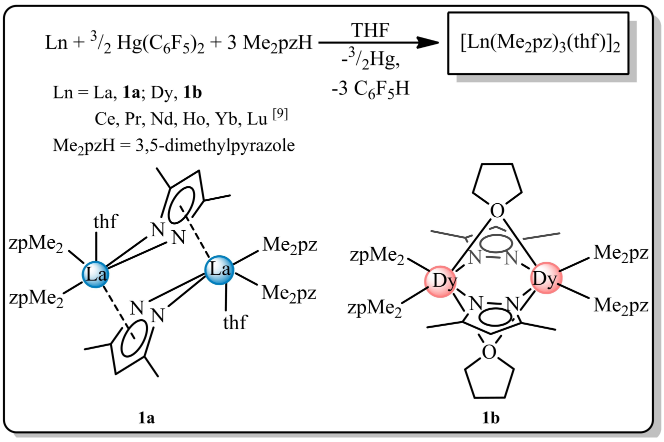

Scheme 1. Synthesis of $[Ln(Me_2pz)_3(thf)]_2$ complexes including (Ln = La (1a) and Dy (1b)).

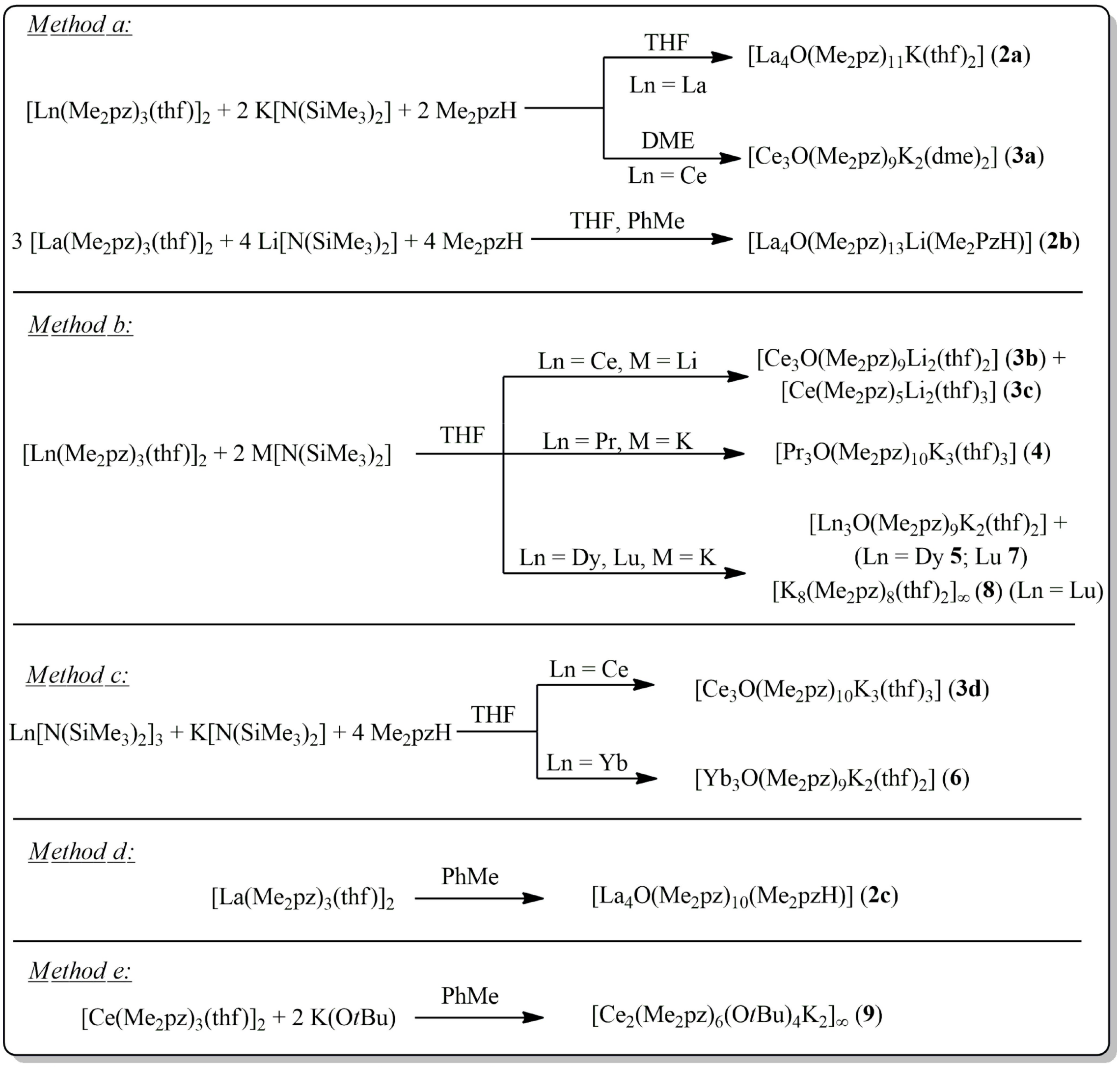

* The stoichiometries are those actually used in the reactions.

Scheme 2. Synthesis of rare-earth pyrazolate oxide cages via different methods.

original suggestion.[1] Because such a small amount of O_2 or H_2O is needed, and given the high reactivity of lanthanoid 3,5-dimethylpyrazolates (see Introduction) and bistrimethylsilylamides, and the need for considerable manipulation in some cases to induce crystal formation, it is certainly impossible to exclude this cause, given the difficulty in total exclusion of small amounts of water by many drying processes.[18–19] The hypothesis is supported by the formation together of the oxido **3 b** and the non-oxido bimetallic **3 c** which was an original target. Water readily coordinates to lanthanoids because of its oxophilic nature, and its small size facilitates bonding. Coordination enhances the acidity hence enabling protolysis of adjacent pyrazolate ligands. The possibility that silicone grease, $(Me_2SiO)_n$ might be the source of oxygen was eliminated by preparing the cages in greaseless Schlenk equipment (see experimental). In any case our focus is on the novelty of the cages and the variety of coordination modes exhibited by the pyrazolate ligands in the cages. As all the reactant complexes have coordinated thf, there is the possibility of de-oxygenation of thf as a source of the cage oxygen as such a reaction can occur with very reactive complexes,[20] but it is less likely as most products still have thf coordinated and some also have thf of crystallization.

X-Ray Structures

A number of new rare earth/alkali metal oxide structures were determined. Representative structures of complexes **2 a**–**8** are shown in Figures 1–10 which also list important bond distances and angles. For all structures carbon atoms are represented as wireframe for clarity. Novel features include five different pyrazolate binding modes in some structures, η^5-K binding is observed in the bimetallic cages in contrast to reported Na/Ln cages[1] and the present Li/Ln cages. Only the second case of a ligand with $\eta^5{:}\eta^5$ donation was observed, incorporated in the

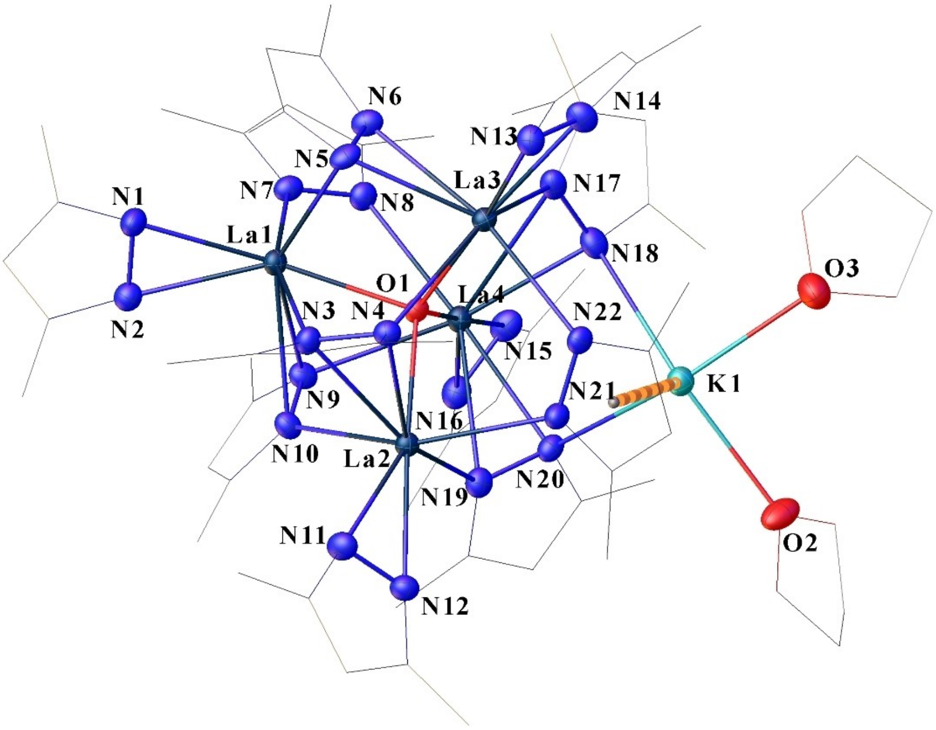

Figure 1. Molecular structure of $[La_4O(Me_2pz)_{11}K(thf)_2]$ (2a). Ellipsoids shown at 50 % probability, hydrogen atoms were removed for clarity.

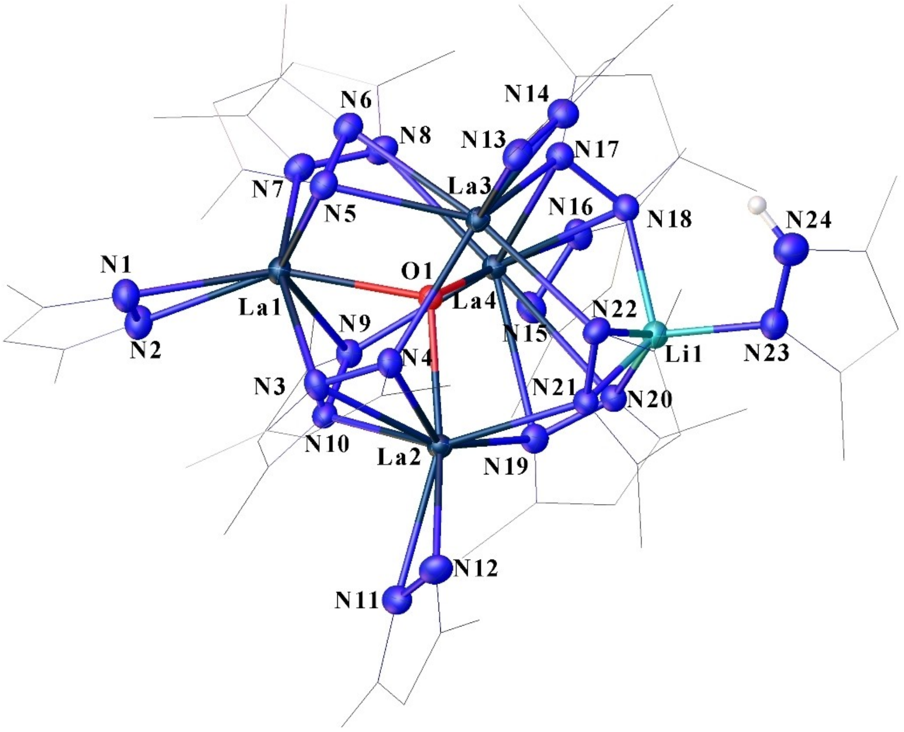

Figure 2. Molecular structure of $[La_4O(Me_2pz)_{11}Li(Me_2pzH)]$ (2b). Ellipsoids shown at 50 % probability, hydrogen atoms were removed for clarity.

new μ_4-1κ(N):2κ(N′):η^5:η^5 binding mode. Selected bond lengths (Å) and angles (°) are shown in Table S1-S4.

$[La_4O(Me_2pz)_{11}K(thf)_2]$ (2 a)

$[La_4O(Me_2pz)_{11}K(thf)_2]$ (**2 a**) crystallises in the triclinic space group *P*-1, with the whole oxide cage within the asymmetric

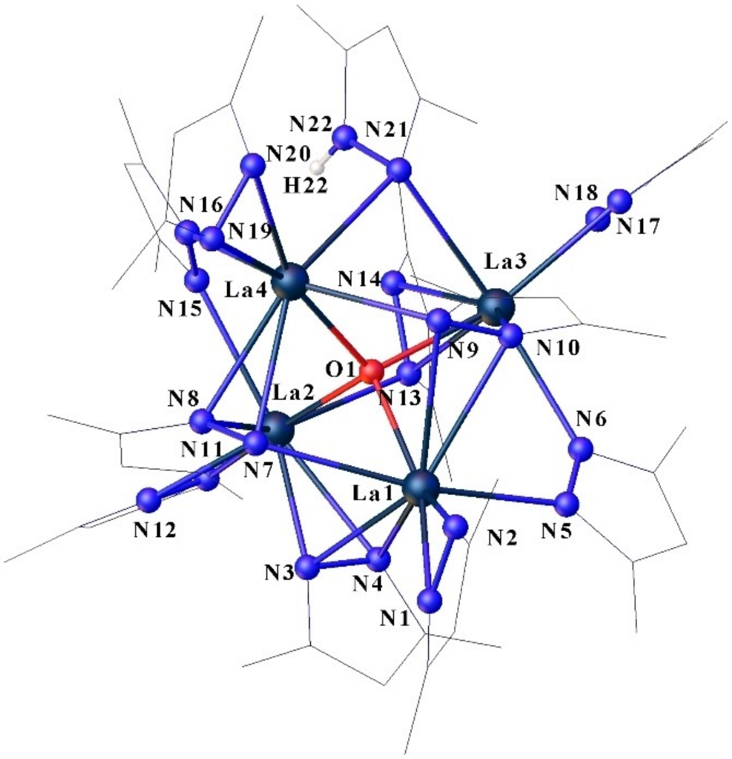

Figure 3. Molecular structure of [$La_4O(Me_2pz)_{10}(Me_2pzH)$] (2c) shown as balls & sticks, hydrogen atoms not assigned except the H of Me_2pzH.

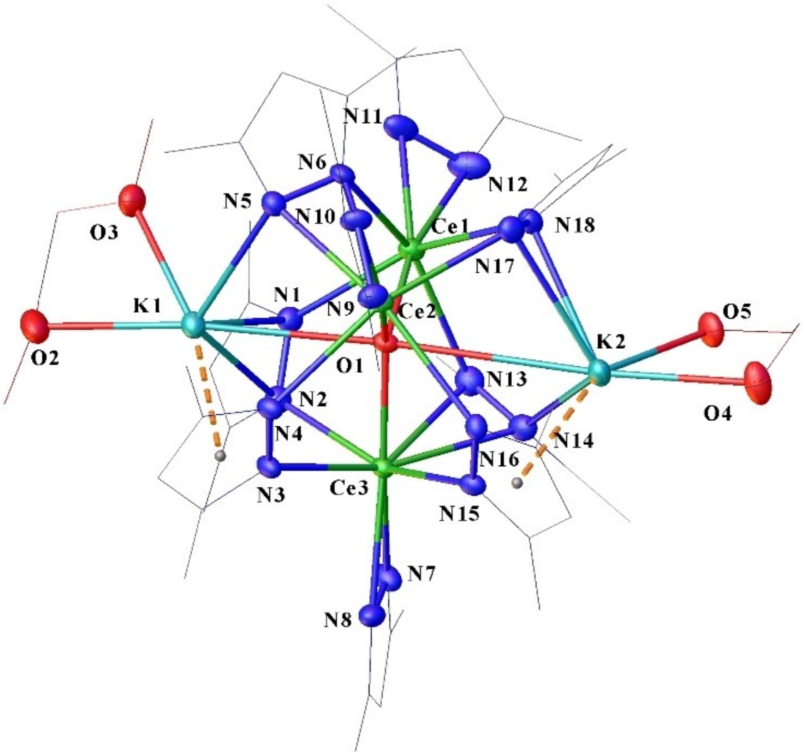

Figure 4. Molecular structure of [$Ce_3O(Me_2pz)_9K_2(dme)_2$] (3a). Ellipsoids shown at 50 % probability, hydrogen atoms removed for clarity.

unit. A cage of four La atoms surrounds a central oxygen in a tetrahedral array, with the potassium atom capping the cage (Figure 1), but not bound to the central oxygen. There are 11 Me_2pz ligands, which adopt a variety of coordination mode: Four N1,2, N11,12, N13,14 and N15,16 chelate (η^2) to La1–4 respectively. Four ligands (N3,4; N9,10; N17,18 and N19,20)

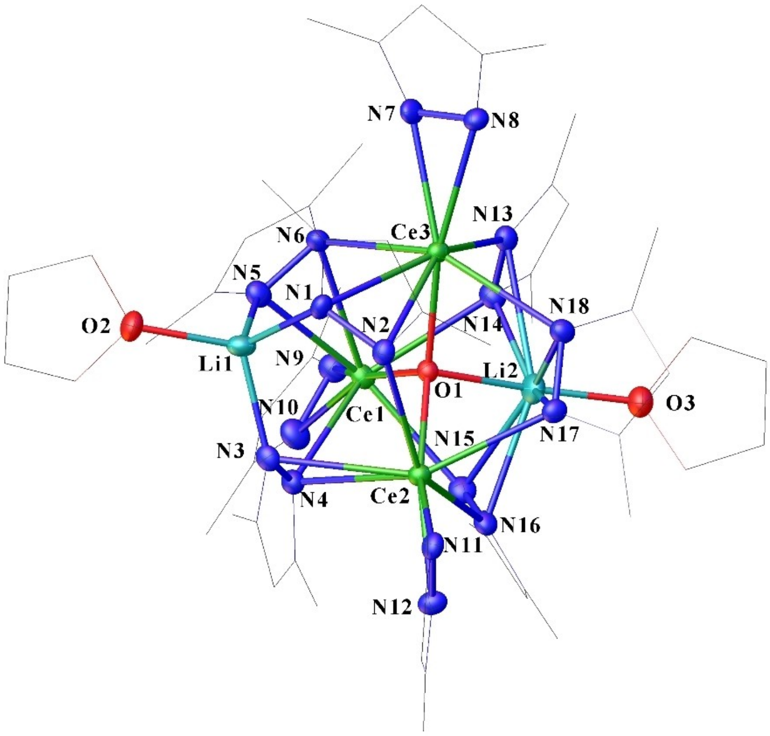

Figure 5. Molecular structure of [$Ce_3O(Me_2pz)_9Li_2(thf)_2$] (3b). Ellipsoids shown at 50 % probability, hydrogen atoms removed for clarity.

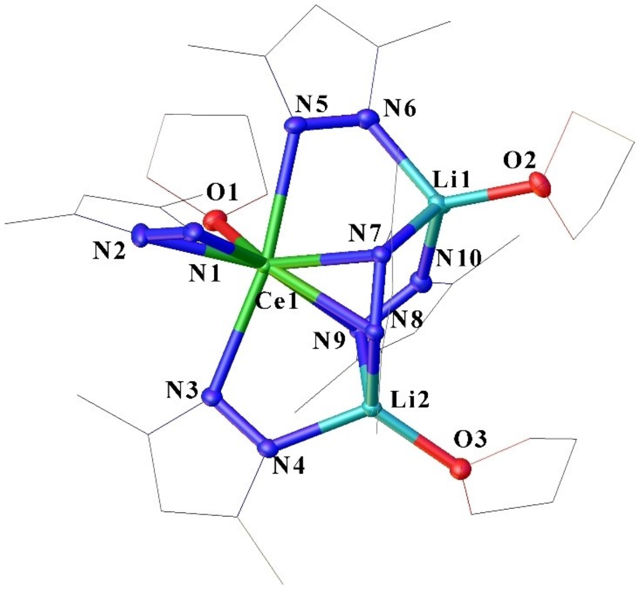

Figure 6. Molecular Structure of [$Ce(Me_2pz)_5Li_2(thf)_3$] (3c). Ellipsoids shown at 35 % probability, hydrogen atoms removed for clarity.

exhibit μ_3-1κ:2η^2:3κ binding and are attached to La1,2,3; La2,1,4; La3,4,K1, and La2,4,K1 respectively. One ligand N5,6 bridges La1,3 in a 1η^2:2η^2 manner and one N7,8 bridges La1,4 in a 1κ(N):2κ(N′) mode. Ligand N21,22 coordinates to La2,3 and K1 in a 1κ:2κ:3η^5 role respectively. Accordingly, La1 and La4 are nine coordinate, while La2 and La3 are eight coordinate. From the foregoing, La1 is bound by O1, N1,2, N3, N5,6, N7, N9,10, La2 by O1, N3,4, N10, N11,12, N19 and N21. La3 by O1, N4, N5,6, N13,14, N17, N22, and La4 by O1, N8, N9, N15,16, La17,18, and N19,20. The capping K1 atom is formally seven coordinate, being bound by O2 and O3 of thf ligands, N18 and N20, and η^5 by the N21,22 C52–54 ligand. The K1-centroid distance is 2.876 Å, which is slightly shorter than K-centroid(tBu_2pz) distance 2.921 Å in [$KLa(tBu_2pz)_4$]·2PhMe.[21]

[$La_4O(Me_2pz)_{11}Li(Me_2pzH)$]·0.5Hexane (2b)

Complex [$La_4O(Me_2pz)_{11}Li(Me_2pzH)$]·0.5Hexane (**2b**) also has a tetrahedral array of La atoms around a central oxygen (Figure 2). The main difference from **2a** lies in the coordination of the smaller (than K) Li atom which caps the cage. As in **2a**, it is coordinated by N20 and N18 of ligands N19,20 and N17, 18, respectively, but ligand N21,22 is η^2 bonded in contrast to η^5 in **2a**. Instead of two thf ligands, there is one unidentate Me_2pzH (N23 of ligand N23,24) leading to overall five coordination for Li in **2b** compared with seven for K in **2a**. Otherwise the coordination environment of La1−4 is as in **2a** with La1,4 nine coordinate and La2,3 eight coordinate.

The five different pyrazolate binding modes of **2a**, **2b** has only been exceeded by the six of [$Ce_4(Me_2pz)_{12}$].[10] Consequently, this complexity complicates comparisons of bond lengths with those of reported La^{III} pyrazolates, which have simpler binding modes. However comparisons can be made of the η^2 and μ-η^2:η^2 bond lengths. **2a** and **2b** have bond lengths for La-N*ter* of η^2-Me_2pz in the narrow range 2.463(3)–2.543(3) Å regardless of whether La is eight or nine coordinate (Table S1). These values are *ca.*0.05 Å larger than terminal La–N of

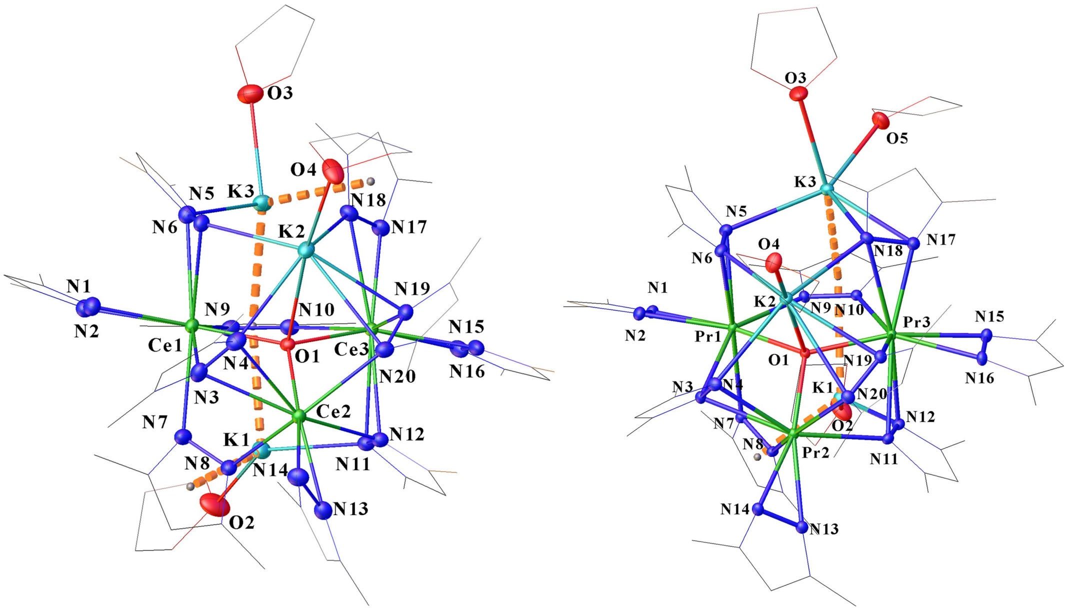

Figure 7. Molecular structures of $[Ce_3O(Me_2pz)_{10}K_3(thf)_3]$ (3 d) (left) and $[Pr_3O(Me_2pz)_{10}K_3(thf)_4]$ (4) (right). Ellipsoids shown at 50 % probability, hydrogen atoms removed for clarity.

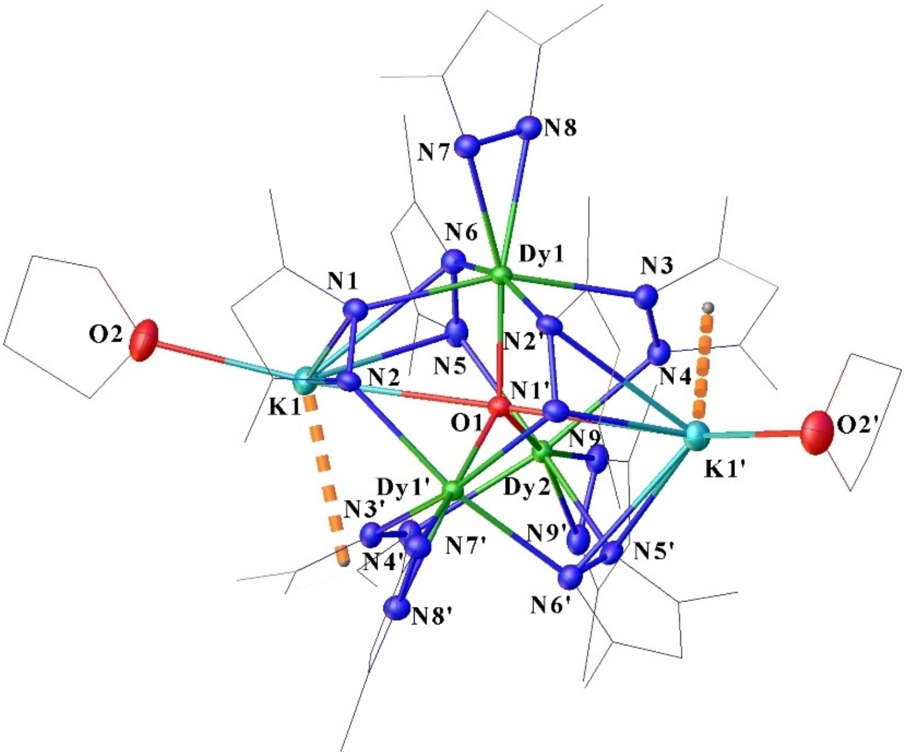

Figure 8. Molecular structure of $[Dy_3O(Me_2pz)_9K_2(thf)_2]\cdot THF$ (5) (representative of Dy, 5, Yb, 6, Lu, 7). Ellipsoids shown at 50 % probability, hydrogen atoms removed for clarity.

$[La_2(tBu_2pz)_6]$,[22] but similar to those of $[K(PhMe)La(tBu_2pz)_4]$.[21] Unsymmetrical μ-η^2:η^2 bonding is observed with La–N of nine coordinate La1 2.757(3)–2.829(3) Å whereas eight coordinate La2 has much shorter La–N bond lengths of 2.507(3)–2.655(5) Å. Eight coordinate $[La_2(tBu_2pz)_6]$ also has unsymmetrical bridging (2.593–2.787(3) Å) in a similar range, but with marked differences in La–N lengths to the same La atom.[22]

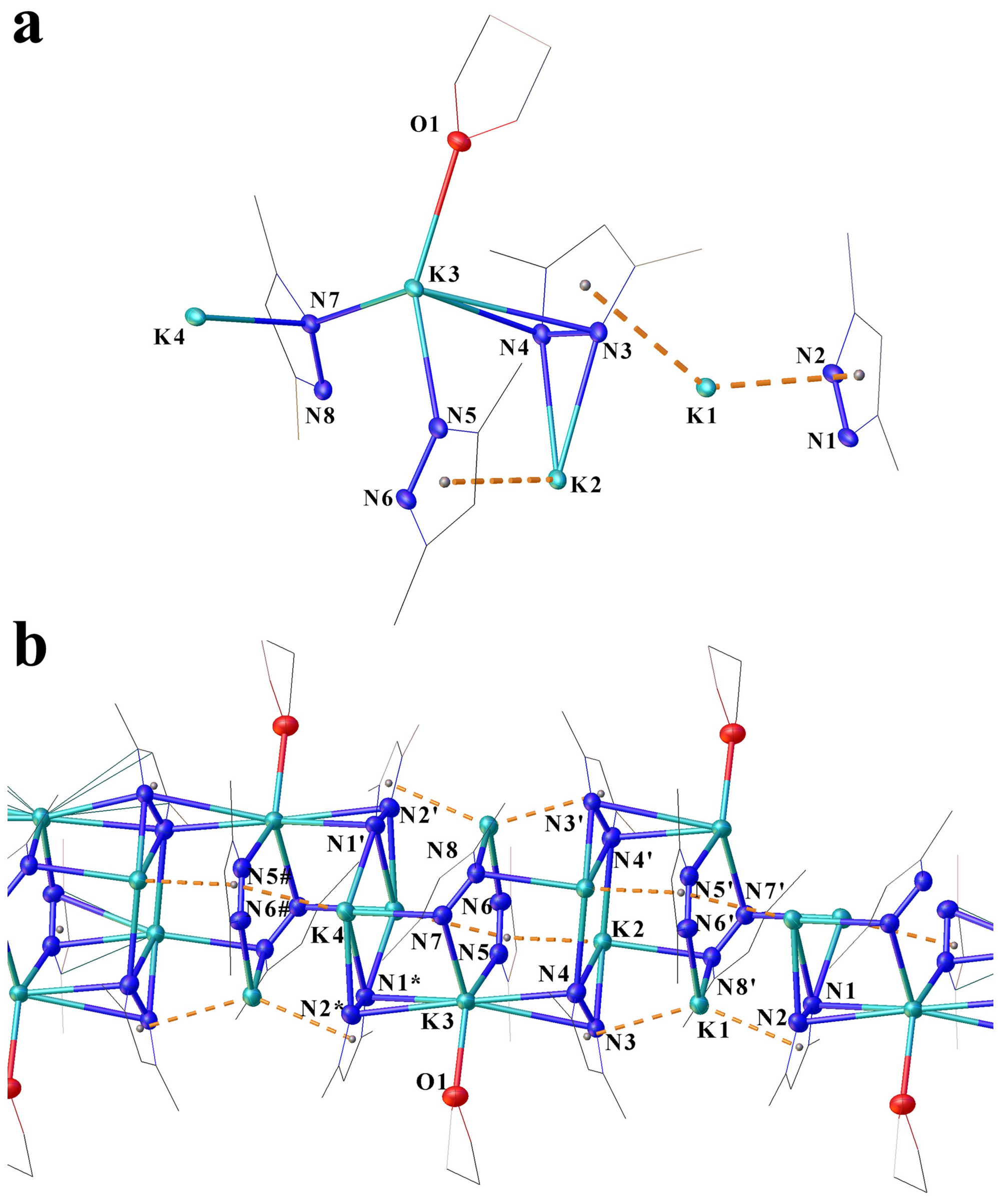

Figure 9. Molecular structure of $\{[K_8(Me_2pz)_8(thf)_2]\cdot THF\}_\infty$ (8) showing (a): the asymmetric unit, (b) along the side of the polymer. Ellipsoids shown at 50 % probability, hydrogen atoms and lattice solvents were removed for clarity. Symmetry code : ′1-X,1-Y,1-Z; *-1+X,+Y,+Z; $^{\#}$-X,1-Y,1-Z. Selected bond lengths (Å): K1-N6′ 2.755(6), K1-N8′ 2.837(6), K1-Cen(N1 N2, C1–3) 2.849, K1-Cen(N3 N4, C7–9) 3.000; K2-N3 2.708(6), K2-N4 2.914(6), K2-N4′ 2.839(6), K2-N8′ 2.826(6), K2-Cen(N5 N6, C12–14) 2.979; K3-N1* 3.088(6), K3-N2* 3.004(6), K3-N3 3.395(6), K3-N4 2.932(6), K3-N5 2.779(6), K3-N7 2.876(6), K3-O1 2.696(5); K4-N1# 2.771(6), K4-N1* 3.030(6), K4-N2* 2.755(6), K4-N7 2.834(6), K4-Cen(N5#N6#, C12#-14#) 2.973.

$[La_4O(Me_2pz)_{10}(Me_2pzH)]$ (2c)

Although small single crystals of **2c** were obtained, they were twinned and only connectivity could be established from the X-ray data. The compound crystallises in the monoclinic space group *C*2/*c* with 1.5 molecules in the asymmetric unit (Figure 3). As with **2a**,**b** there is a tetrahedron of lanthanum atoms around a central oxygen. The most novel feature is that the single 3,5-dimethylpyrazole ligand is coordinated to two lanthanum atoms La3,4 through the single nitrogen N21 in a 1κ(N):2κ(N) manner. Although there are a few examples of a pyridine ligand bridging two metals though a single lone pair,[23–24] this appears not to have been observed for the aromatic nitrogen of pyrazole.

In **2c**, La1 is coordinated by the central oxygen (O1), a terminal Me_2pz (N1 N2), N3,N4 of μ_2-η^2:η^2 and N9,N10 of μ_3-1η^2:2κ(N):3κ(N′) ligands, N5 from a μ_2-1κ(N):2κ(N′) ligand, and N7 from a μ_3-1κ(N):2η^2:3κ(N′) ligand. La2 is bound by O1, a chelating pyrazolate (N11,N12), N3,N4 of a μ-η^2:η^2-Me_2pz, N8 of a μ_3-1κ(N):2η^2:3κ(N′) ligand, N13 of a μ_2-1κ(N):2η^2 ligand, and N15 from a μ_2-1κ(N):2κ(N′) ligand. La3 is coordinated by the central oxygen (O1), a terminal Me_2pz (N17 N18), and N6, N9, N13, N14 of the various bridging Me_2pz ligands, and N21 of the Me_2pzH ligand. La4 is bound by O1, a chelating pyrazolate (N19 N20), and N7, N8, N9, and N16 of the various bridging

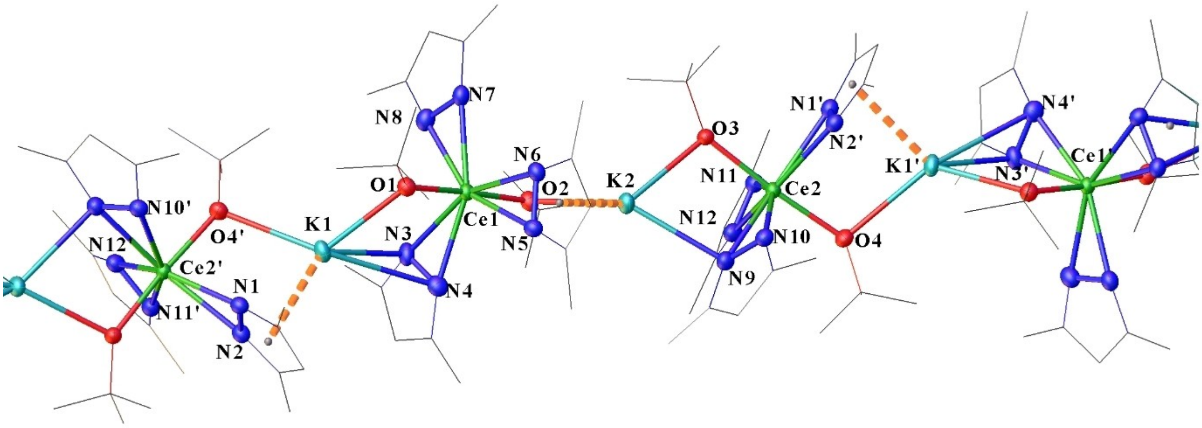

Figure 10. Molecular structure of $[Ce_2(Me_2pz)_6(OtBu)_4K_2]_\infty$ (9). Ellipsoids shown at 50 % probability, hydrogen atoms removed for clarity. Symmetry generated atoms shown as black. Selected bond lengths (Å, left to right) for 9: K1-O4′ 2.801(3), K1-O1 2.763(3), K1-N3 2.815(4), K1-N4 3.136(4), K1-Cen(N1 N2, C4–6) 2.883, Ce1-O1 2.150(3), Ce1-O2 2.143(3), Ce1-N3 2.480(3), Ce1-N4 2.449(4), Ce1-N5 2.474(4), Ce1-N6 2.453(4); Ce1-N7 2.396(4), Ce1-N8 2.398(3); K2-O2 2.789(3), K2-O3 2.737(3), K2-N9 2.819(4), K2-Cen(N5 N6, C18–20) 2.877; Ce2-O3 2.153(3), Ce2-O4 2.148(3), Ce2-N1′ 2.470(3), Ce2-N2′ 2.445(3), Ce2-N9 2.476(4), Ce2-N10 2.439(3), Ce2-N11 2.401(3), Ce2-N12 2.426(4).

Me_2pz ligands, and N21 of the Me_2pzH ligand. Thus, only La1 is nine coordinate with La2–4 eight coordinate. There are five different Me_2pz coordination modes in addition to the new pyrazole mode.

$[Ce_3O(Me_2pz)_9K_2(dme)_2]$ 3 a

Compound **3 a** crystallises in the orthorhombic space group $Pna2_1$, with the whole molecule occupying the asymmetric unit (Figure 4). Three cerium atoms surround the central oxygen atom, with the cage being capped at the axial positions by K(dme) units. Weak K1-O1 interactions at 3.271(4) Å, and K2-O1 at 3.678(4) Å (Table S2) are within the sum (4.25 Å) of the van der Waals radii of potassium and oxygen.[25–26] The Ce_3O geometry of the central oxygen atom is almost trigonal planar, with only a minor influence by the capping potassium atoms. This results in an elongated trigonal bipyramid of metal atoms surrounding oxygen. Each cerium atom has one terminal Me_2pz ligand, whereas all the other six Me_2pz ligands are bridging between three metal atoms, two being 1κ(N):2κ(N′) between Ce atoms and η^5 bound to K1 or K2, and four 1κ(N):2κ(N′):η^2, with chelation to Ce2, Ce3, K1 or K2 by the various ligands.

Ce1 is seven coordinate, and Ce2 and Ce3 are eight coordinate. Ce1 is bound by four bridging κ(N) Me_2pz ligands (N1,6,13,18), one terminal η^2 Me_2pz ligand (N11 N12), and one bridging oxide ligand (O1). Ce2 and Ce3 are bound by one bridging η^2 Me_2pz ligand (N5 N6 for Ce2; N13 N14 for Ce3), three bridging κ(N) Me_2pz ligands (N4,16,17 for Ce2; N2,3,15 for Ce3), and one terminal η^2 Me_2pz ligand (N9 N10 for Ce2; N7 N8 for Ce3), and one bridging oxide ligand (O1). K1 and K2 are nine coordinate. Both K atoms are bound by one bridging η^5-Me_2pz ligand (N3,4 C7–9 for K1, N15,16 C37–39 for K2), one bridging η^2-Me_2pz ligand (N1,2 for K1, N17,18 for K2), one bridging κ(N)-Me_2pz ligand (N5 for K1, N14 for K2), one terminal dme ligand (O2O3 for K1, and O4O5 for K2), and one bridging oxide ligand (O1). The K-centroid distances of the η^5 bound pyrazolate are *ca.* 0.1 Å longer than in **2 a**, but the metal coordination number is two higher in **3 a** leading to the longer contacts.

$[Ce_3O(Me_2pz)_9Li_2(thf)_2]$ (3 b)

Whilst the composition of $[Ce_3O(Me_2pz)_9Li_2(thf)_2]$ (3b) is similar to those of reported $[Ln_3O(Me_2pz)_9Na_2(thf)_2]$ (Ln = Y, Ho, Yb, Lu)[1] complexes, the similarity ends there, as the structure of 3b is quite different. It crystallises in the triclinic space group P-1, with the whole molecule within the asymmetric unit (Figure 5). A triangle of Ce atoms surrounds a central oxygen with lithium atoms capping a distorted trigonal bipyramid. Li2-O1 is a comparatively short bond, but the Li1….O1 distance is near the sum of the van der Waals radii of lithium and oxygen,[25] outside the sum of the radii if the Bondi value for lithium is used,[25] and is ca. 1.5 Å longer than Li2-O1, hence is probably only a non-bonding van der Waals contact. Further Li1 is four coordinate with short Li–N bonds (below), whilst Li2 is surprisingly eight coordinate but with relatively long Li2-N bonds. Of the nine pyrazolate ligands, three (N9,10, N11,12, and N,7,8) are terminal η^2, and bind to Ce1,2,3 respectively. The others are all bound to three metals in a 1κ:2η^2:3κ manner. Thus N1,2 chelates Ce3, and is unidentate N1Li1 and N2Ce2, N3,4 chelates Ce2 and is unidentate in N3Li1 and N4Ce1, N5,6 chelates Ce1, and is unidentate in N5Li1 and N6Ce3; N13,14 chelates Li2 and is unidentate in N13Ce3 and N14Ce1, N15,16 chelates Li2 and is unidentate in N15Ce1 and N16Ce2, whilst N17,18 also chelates Li2 and is unidentate in N17Ce2 and N18Ce3.

$[Ce(Me_2pz)_5Li_2(thf)_3]$ (3 c)

Trimetallic 3c crystallises in the monoclinic space group $P2_1/n$, with the whole molecule within the asymmetric unit, and is not an oxide cage (Figure 6). The eight coordinate cerium atom is coordinated by one terminal η^2-Me_2pz (N1 N2) and one terminal thf ligand (O1), with four Me_2pz ligands bridging to one or both Li atoms in either a μ_2-1κ(N3/N5):2κ(N4/N6), μ_3-1κ(N9):2κ(N9):3κ(N10), or μ_3-1η^2(N7,N8):2κ(N7):3κ(N8) fashion. Li1 and Li2 are four coordinate, by three bridging Me_2pz ligands (N6,7,10 for Li1, N4,8,9 for Li2), and one terminal thf ligand (O2 for Li1, O3 for Li2).

$[Ce_3O(Me_2pz)_{10}K_3(thf)_3]$ (3 d) and $[Pr_3O(Me_2pz)_{10}K_3(thf)_4]$ (4)

The closely related complexes $[Ce_3O(Me_2pz)_{10}K_3(thf)_3]$ (3 d) and $[Pr_3O(Me_2pz)_{10}K_3(thf)_4]$ (**4**), which differ mainly in the number of thf ligands attached to one potassium, crystallize in the monoclinic space group *P*2$_1$, and the orthorhombic space group *P*2$_1$2$_1$2$_1$, respectively (Figure 7). Each contains an approximately tetrahedral KLn_3 core bound to a central oxygen atom. This forms part of a larger K_3Ln_3 cage, in which the K1-O1 and K3-Ln3 distances are considered too long to be bonding.

In **3 d** (Figure 7 left), Ce1 and Ce2 are eight coordinate, and Ce3 is nine coordinate. Ce 1, Ce2 and C3 are each coordinated by one terminal η^2 Me_2pz ligand (N1 N2, N13 N14, and N15 N16, respectively). Four ligands (N3,4, N5,6, N11,12, N19,20) bind in a 1κ:2η^2:3κ manner. They chelate to Ce2, Ce1, Ce3, and K2 respectively, and attach as unidentates to Ce1 and 2, K3 and 2, K1 and Ce2, and Ce3 and 2, respectively. The remaining ligands N7,8, N9,10, and N17,18 have different binding modes but each has at least one η^5-K interaction. N7,8 has N7 bound to Ce1, N8 to Ce2, and an η^5-K1 interaction. N17,18 has μ_3-1κ(N):η^2:η^5 coordination to K2, Ce3 and K3 respectively. N9,10 has μ_4-1κ(N):2κ(N′):η^5:η^5 ligation, being bound to Ce1, K2, K1 and K3 respectively with a K1-cen-K3 angle of 139° (Table S3). It appears to be the first observation of this binding mode. The only other example of double η^5 donation by a single pyrazolate ligand is in $[(Me_2pzH)(Me_2pz)_2(18\text{-crown-}6)(thf)K_2]_2$ where the binding is μ_3- η^5: η^5: η^2 and the K-cen-K angle is 167°.[27]

In the praseodymium complex **4** (Figure 7 right), the coordination numbers of the metals are the same as in **3 d**, and the binding modes of the ligands and the coordination environment are unchanged except for N17,18 and K3. Thus, ligand N17,18 binds η^2 to K3 in **4** in contrast to η^5 in **3 b**, and is overall attached μ_3–1κ:2η^2:3η^2. Eight coordination of K3 is maintained by two thf ligands compared with one in **3 d**.

$[Ln_3O(Me_2pz)_9K_2(thf)_2]$ (Ln = Dy, 5, Yb, 6, Lu, 7)

Complexes $[Dy_3O(Me_2pz)_9K_2(thf)_2]\cdot THF$ (**5**), $[Yb_3O(Me_2pz)_9K_2(thf)_2]\cdot THF$ (**6**) and $[Lu_3O(Me_2pz)_9K_2(thf)]\cdot THF$ (**7**) crystallise in the orthorhombic space group *P*bcn, with half a molecule in the asymmetric unit. They are isomorphous, having similar unit cell parameters.

In **5** (Figure 8), all three Dy atoms are seven coordinate, and both K atoms are nine coordinate. Of the five unique Me_2pz ligands, two are terminal η^2 (N7,8; N9,9′), two are 1κ:2η^2:3κ binding (N1,2; N5,6) and one is 1κ:2κ:η^5 (N3,4). The three Dy atoms are bound by four bridging κ(N) Me_2pz ligands, one terminal η^2 Me_2pz ligand and one bridging oxide ligand (O1). Two K atoms are bound by two bridging η^2 Me_2pz ligands, one bridging η^5-Me_2pz ligand, one terminal thf ligand and one bridging oxide ligand (O1).

The average Ln–N bond lengths of the terminal pyrazolate ligands, of the 1κ:2η^2:3κ pyrazolates, and of 1κ:2η^5:3κ pyrazolate ligands to Dy, Yb, Lu are 2.388, 2.345, 2.344 Å; 2.473, 2.426, 2.414 Å, and 2.505, 2.456, 2.441 Å (Table S4), respectively. All show the effects of the Ln contraction. Although the complexes have a similar stoichiometry to Schumann's disodium analogues, the pyrazolate binding is completely different.

$\{[K_8(Me_2pz)_8(thf)_2]\cdot THF\}_\infty$ (8)

Complex **8** crystallises in the triclinic space group *P*-1 as a 1-D polymer, and half the molecular formula is present in the asymmetric unit (Figure 9). The structure indicates a complex framework, wherein each Me_2pz ligand is coordinating to multiple potassium ions in three different coordination modes, including the new (see **3 d** and **4**) μ_4–1κ:2κ:3η^5:4η^5-Me_2pz. The only other group one Me_2pz complex known is the tetrameric $[Na_4(Me_2pz)_4(thf)_4]$.[28–29] This complex differs from **8** as it is a discrete molecule, where each Me_2pz unit is bridged between three sodium atoms through either η^2 or κ^1 interactions.

K1 is eight coordinate, and K2, K3, K4 are seven coordinate. K1 is bound by two bridging η^5 Me_2pz ligands (N1 N2, C1–3 and N3 N4, C7–9) and two nitrogen atoms (N6′, N8′) from μ_4–1κ:2κ:3η^5:4η^5- and μ_4–1κ:2κ:3κ:4κ-Me_2pz ligands, respectively. K2 is bound by one bridging η^5 Me_2pz ligand (N5 N6, C12–14), two nitrogen atoms (N4′, N8′) from one 1κ:2η^2:3η^2:4η^5-Me_2pz and one μ_4–1κ:2κ:3κ:4κ-Me_2pz ligand and η^2 (N3 N4) from a 1κ:2η^2:3η^2:4η^5 ligand, K3 is bound by two nitrogen atoms (N5, N7) from μ_4–1κ:2κ:3η^5:4η^5- and μ_4–1κ:2κ:3κ:4κ-Me_2pz ligands respectively, two η^2 from two μ_4–1κ:2η^2:3η^2:4η^5-Me_2pz ligands (N1*N2*, N3 N4), and one terminal thf ligand (O1), K4 is bound by one bridging η^5 Me_2pz group from the μ_4–1κ:2κ:3η^5:4η^5 ligand (N5#N6#, C12#-14#), two nitrogens (N1′, N7) from μ_4–1κ:2η^2:3η^2:4η^5- and μ_4–1κ:2κ:3κ:4κ-Me_2pz ligands and one η^2 (N1*N2*) group from a μ_4–1κ:2η^2:3η^2:4η^5 ligand.

$[Ce_2\ (Me_2pz)_6(OtBu)_4K_2]_\infty$ (9)

Complex **9** is a cerium(IV) 1-D bimetallic polymer which crystallises in the monoclinic space group *P*2$_1$/c, with the repeating group occupying the asymmetric unit (Figure 10). All metals in the sequence K1Ce1 K2Ce2 K1′ are bridged by *t*BuO groups with K1 and Ce1 also bridged by an η^2:η^2-Me_2pz (N3,4), Ce1 and K2 by an η^2:η^5-Me_2pz (N5,6), K2 and Ce2 by a 1κ(N9):η^2-Me_2pz (N9,10), and Ce2 and K1′ by an η^2:η^5-Me_2pz (N1,2). Both Ce1 and Ce2 are eight coordinate. Each has a terminal η^2-Me_2pz ligand (N7,8; N11,12 respectively), two bridging η^2-Me_2pz (N3,4; N5,6 for Ce1; N1′,2′; N9,10 for Ce2), and two bridging *tert*-butoxide donors. Besides two bridging alkoxide ligands, K1 has η^5-(N1,2) and η^2-(N3,4)-Me_2pz ligands and K2 has a bridging η^5 (N5,6)-, and a bridging 1κ(N12)-Me_2pz′. The terminal Ce–N bond lengths of the terminal pyrazolate ligands to cerium ave. 2.41 Å, (2.396(4)–2.426(4) Å) are at the high end of the range for two homoleptic Ce^{IV} pyrazolates, namely $[Ce(Me_2pz)_4]_2$ and [Ce-

(tBu$_2$pz)$_4$] (2.311(2)-2.400(2) Å).[11] On the other hand, the Ce–N bonds of bridging η^2-Me$_2$pz groups of **9** (2.439(3)-2.480 Å) are at the low end of and cover a much narrower range than those of [Ce(Me$_2$pz)$_4$]$_2$ (2.473(2)-2.703(2) Å).[11] Cerium(IV) pyrazolates are rare and have only recently been reported.[11,14]

Conclusions

A wide range of oxide cage complexes has been synthesised with both hetero-bimetallic and homometallic constitutions from trivalent rare-earth 3,5-dimethylpyrazolate complexes, [Ln(Me$_2$pz)$_3$(thf)]$_2$ (Ln = La, Ce, Pr, Dy, Yb, Lu) using four different routes. The oxide source is considered to be adventitious water or oxygen, of which only trace amounts are needed to achieve the outcomes. The Ln$_n$ cage size is lanthanoid ion radius dependent with n = 4 observed solely for the largest lanthanoid La. In all other cases n = 3. Striking features of the structures include as many as five different pyrazolate binding modes in some cases, a new pyrazolate binding mode that includes η^5 bridging two metals, and a single pyrazole nitrogen bridging two metals. Such results indicate this area contains rich potential that warrants further investigation.

Experimental

General

All products are air-sensitive and required manipulation in an inert atmosphere using glovebox, Schlenk flask and vacuum line techniques. All solvents were pre-dried with sodium metal and then further dried by distillation over sodium or sodium/benzophenone. The lanthanoid metals used were purchased either from Rhône-Poulenc or Santoku either as fine powders or as metal ingots which were manually filed into metal filings in an inert atmosphere for use in the reactions. 3,5-Dimethylpyrazole (Me$_2$pzH) and K[N(SiMe$_3$)$_2$] were purchased from Aldrich/Sigma-Aldrich. {Ln[N(SiMe$_3$)$_2$]$_3$} (Ln = Ce, Yb) complexes were synthesised by treatment of THF activated LnCl$_3$ with three equivalents of K[N(SiMe$_3$)$_2$] in hexane, and were purified by filtration, evaporation to dryness (*in vacuo*), and re-crystallisation from fresh hexane. Microanalyses were performed by the elemental analysis service of London Metropolitan University, or analysed with an 'elementar vario MICRO cube' by Mr. Stephen Boch of Tübingen University. Listed infrared data are of Nujol mulls for the region 4000–650 cm^{-1} using a Perkin Elmer 1600 FTIR spectrometer. Alternatively, crystals immersed in crystallography oil were measured on an Aglient Cary 630 FTIR ATR instrument. ^{1}H-NMR spectra were recorded with a Bruker DRX400 (400 MHz) spectrometer, or a Bruker DRX300, however, no meaningful spectra could be obtained for paramagnetic complexes. [Ln(Me$_2$pz)$_3$(thf)]$_2$ (Ln = La, Ce, Pr, Yb, Lu) complexes were prepared as reported.[9] Crystals were measured on an Oxford Gemini ultra diffractometer, a 'Bruker P4' diffractometer or the MX1 beamlines at the Australian Synchrotron. Crystal data and refinement details are given in SI. Deposition Numbers CCDC 2373572–2373573 for compounds **1a–1b**, 2373574–2373575 for compounds **2a–2b**, 2373576–2373579 for compounds **3a-3d**, 2373580–2373585 for compounds **4–9**, contain the supplementary crystallographic data for this paper. These data are provided free of charge from The Cambridge Crystallographic Data Centre via www.ccdc.cam.ac.uk/data request/cif.

[La(Me$_2$pz)$_3$(thf)] 1 a

The crystal structure was not previously reported, only the unit cell, owing to crystal quality.[9] **1a** was dissolved in a THF/hexane mixture and allowed to slowly evaporate. After the solution was concentrated (~0.5 mL) the flask was deliberately agitated, producing small clear needles.

[Dy(Me$_2$pz)$_3$(thf)]$_2$ 1 b

Dysprosium metal (0.28 g, 1.7 mmol), Hg(C$_6$F$_5$)$_2$ (1.40 g, 2.60 mmol), and Me$_2$pzH (0.50 g, 5.2 mmol) were stirred in THF (15 mL) (**in a greaseless Schlenk flask**) for two days. After filtration from the metal residues and evaporation to dryness (*in vacuo*), [Dy(Me$_2$pz)$_3$(thf)]$_2$ was crystallised from a hot THF solution yielding block crystals of [Dy(Me$_2$pz)$_3$(thf)]$_2$. Crystal yield = 0.35 g (38 %); Elemental analysis calcd. (%) for: C$_{38}$H$_{58}$Dy$_2$N$_{12}$O$_2$ (1039.96): C 43.89, H 5.62, N 16.16; found: C 43.67, H 5.78, N 15.94.

Synthesis of Rare-Earth Oxide Complexes

All experiments were conducted in Schlenk flasks with silicone greased fittings unless stated otherwise.

[La$_4$O(Me$_2$pz)$_{11}$K(thf)$_2$] (2 a)

[La(Me$_2$pz)$_3$(thf)]$_2$ (0.28 g, 0.28 mmol), K[N(SiMe$_3$)$_2$] (0.11 g, 0.56 mmol), and Me$_2$pzH (0.53 g, 0.56 mmol) were stirred in THF (3 ml) for two days. The sample was dried (*in vacuo*) and hexane/THF was added. The solution was stored in the freezer (at -20°C), and block crystals of [La$_4$O(Me$_2$pz)$_{11}$K(thf)$_2$] (**2a**) formed overnight, with composition identified by X-ray crystallography.

[La$_4$O(Me$_2$pz)$_{11}$Li(Me$_2$pzH)]·0.5Hexane (2 b):

[La(Me$_2$pz)$_3$(thf)]$_2$ (0.44 g, 0.44 mmol), Li[N(SiMe$_3$)$_2$] (0.098 g, 0.59 mmol) and Me$_2$pzH (0.060 g, 0.62 mmol) were stirred in THF (5 mL), the solution was evaporated to dryness (*in vacuo*) and PhMe was added. A slow evaporation process produced a thick light yellow oil, hexane was added, and after four days the solution was evaporated *in vacuo*. Fresh hexane was added and the sample produced block crystals of [La$_4$O(Me$_2$pz)$_{11}$Li(Me$_2$pzH)]·0.5Hexane (**2b**), with the identity determined by X-ray crystallography. Crystal yield = 0.20 g (53 %); Elemental analysis calcd. (%) for C$_{63}$H$_{92}$La$_4$LiN$_{24}$O (M = 1764.18): C 42.89, H 5.26, N 19.06; C$_{60}$H$_{85}$La$_4$LiN$_{24}$O (1721.04, hexane of crystallisation lost): C 41.87, H 4.98, N 19.53; found: C 41.93, H 5.15, N 19.63.

[La$_4$O(Me$_2$pz)$_{10}$(Me$_2$pzH)] (2 c):

Crystals of [La(Me$_2$pz)$_3$(thf)]$_2$ were heated in PhMe. After several days the solution was allowed to slowly cool, giving small crystals of [La$_4$O(Me$_2$pz)$_{10}$(Me$_2$pzH)] (**2c**), though crystal data was poor due to the crystals decomposing within the X-ray beam (at the Australian Synchrotron) monoclinic, space group C2/c, unit cell: a 67.302(14), b 13.166(3), c 22.339(5), α, γ = 90, β = 93.35(3). Elemental analysis calcd (%) for: C$_{55}$H$_{78}$La$_4$N$_{22}$O (1618.97): C 40.80, H 4.86, N 19.03; found: C 40.68, H 4.77, N 18.91.

[Ce$_3$O(Me$_2$pz)$_9$K$_2$(dme)$_2$] (3 a):

[Ce(Me$_2$pz)$_3$(thf)]$_2$ (0.092 g, 0.10 mmol), K[N(SiMe$_3$)$_2$] (0.036 g, 0.18 mmol) and Me$_2$pzH (0.017 g, 0.18 mmol) were dissolved in DME (5 mL), a slight bubbling was noticed immediately upon solvent addition. After 24 hours of stirring at ambient temperature the reaction solution was dried in vacuo, and fresh DME was added with hexane layering. Storage overnight yielded light colourless block crystals of $[Ce_3O(Me_2pz)_9K_2(dme)_2]$ (**3a**), with the identity determined by X-ray crystallography.

$[Ce_3O(Me_2pz)_9Li_2(thf)_2]\cdot 0.5$Hexane (3b) and $[Ce(Me_2pz)_5Li_2(thf)_3]$ (3c)

$[Ce(Me_2pz)_3(thf)]_2$ (0.020 g, 0.02 mmol), $Li[N(SiMe_3)_2]$ (0.02 g, 0.11 mmol), and Me_2pzH (0.012 g, 0.11 mmol) were dissolved in THF (**in a greaseless Schlenk flask**) and the solution allowed to slowly evaporate. After several weeks small crystals of both $[Ce_3O(Me_2pz)_9Li_2(thf)_2]$ (**3b**) and $[Ce(Me_2pz)_5Li_2(thf)_3]$ (**3c**) formed, where the identity of both compounds was determined by X-ray crystallography.

$[Ce_3O(Me_2pz)_{10}K_3(thf)_3]$ (3d):

$Ce[N(SiMe_3)_2]_3$ (0.060 g, 0.10 mmol), $K(Me_2pz)$ (0.02 g, 1.0 mmol), and Me_2pzH (0.036 g, 0.37 mmol) were stirred in THF (3 mL) for two days. The mixture was evaporated to dryness (in vacuo), and fresh THF/hexane was added (~2:2 mL). After one day small crystals of $[Ce_3O(Me_2pz)_{10}K_3(thf)_3]$ (3d) were deposited on the surface of the sample vial, with the identity determined by X-ray crystallography. Crystal yield =0.03 g (54%). The supernatant solution was removed, and the crystals were dried in vacuo. Elemental analysis calcd. (%) for $C_{62}H_{94}Ce_3K_3N_{20}O_4$ (1721.23): C 43.26, H 5.51, 16.28; $C_{67}H_{102}Ce_3K_3N_{22}O_4$ (1817.31, containing a molecule of Me_2pzH in the bulk sample): C 44.28, H 5.66, 16.96; found: C 44.88, H 5.99, N 16.65.

$[Pr_3O(Me_2pz)_{10}K_3(thf)_3]$ (4):

$[Pr(Me_2pz)_3(Thf)]_2$ (0.051 g, 0.06 mmol) and $K[N(SiMe_3)_2]$ (0.022 g, 0.11 mmol) were stirred in THF for two days. The solution was concentrated (*in vacuo*) and hexane was layered, producing thick block crystals of $[Pr_3O(Me_2pz)_{10}K_3(thf)_3]$ (**4**). The composition was determined by X-ray crystallography.

$[Dy_3O(Me_2pz)_9K_2(thf)_2]\cdot$THF (5):

$[Dy(Me_2pz)_3(thf)]_2$ (0.25 g, 0.24 mmol) and $K[N(SiMe_3)_2]$ (0.096 g, 0.48 mmol) were stirred in THF (5 mL) (**in a greaseless Schlenk flask**) with heating (~50 °C) for two days. Hexane was added and the solution required further heating to avoid precipitation of the reactant. Upon slow cooling of the reaction mixture small crystals were produced $[Dy_3O(Me_2pz)_9K_2(thf)_2]\cdot$THF (**5**). Yield = ~0.10 g (38%). Elemental analysis calcd. (%) for: $C_{57}H_{87}Dy_3K_2N_{18}O_4$ (M = 1654.14): C 41.39, H 5.30, N 15.24; $C_{53}H_{79}Dy_3K_2N_{18}O_3$ (1582.01, THF of crystallisation lost): C 40.24, H 5.03, N 15.93; found: C 40.33, H 5.16, N 15.88.

$[Yb_3O(Me_2pz)_9K_2(thf)_2]\cdot$THF (6):

$Yb[N(SiMe_3)_2]_3$ (0.05 g, 0.08 mmol), $K[N(SiMe_3)_2]$ (0.015 g, 0.076 mmol) and Me_2pzH (0.029 g, 0.30 mmol) were stirred in THF (3 mL) for two days resulting in a light-yellow solution. The mixture was evaporated to dryness in vacuo, fresh THF (~1 mL) was added with additional hexane layering (0.5 mL). Storage at −35 °C overnight afforded small block crystals of $[Yb_3O(Me_2pz)_9K_2(thf)_2]\cdot$THF (**6**). The composition was determined by X-ray crystallography.

$[Lu_3O(Me_2pz)_9K_2(thf)_2]\cdot$THF (7) and $\{[K_8(Me_2pz)_8(thf)_2]\cdot\text{THF}\}_\infty$ (8):

$[Lu(Me_2pz)_3(thf)]_2$ (0.30 g, 0.56 mmol) and $K[N(SiMe_3)_2]$ (0.11 g, 0.55 mmol) were stirred in THF (~2–3 mL) for two days. The solvent was removed (in vacuo), and the colourless powder was dissolved in a THF hexane (~1:1 mL) mixture. After the solution was heated and allowed to slowly cool (to room temperature), small block crystals were isolated of $[Lu_3O(Me_2pz)_9K_2(thf)_2]\cdot$THF (**7**). Crystal yield = 0.25 g (80%); ^{1}H NMR (C_6D_6, 333.2 K): δ = (resonances around 0.09–0.29 with integrations of less than 10% are not included, see Figure S1), 1.42 (m, 10 H, β-thf), 1.98 (s, 36 H, CH_3), 2.30 (s, 18 H, CH_3), 3.56 (m, 10 H, α-thf), 5.61 (s, 6 H, H4-Me_2pz), 6.47 ppm (s, 3 H, H4-Me_2pz) with 0.5 thf of crystallisation lost; Elemental analysis calcd. (%) for: $C_{57}H_{87}K_2Lu_3N_{18}O_4$ (M = 1691.55): C 40.47, H 5.18, N 14.91; $C_{53}H_{79}K_2Lu_3N_{18}O_3$ (1619.41, THF of crystallisation lost): C 39.31, H 4.92, N 15.57; found: C 39.40, H 4.89, N 15.39. Small colourless block crystals of $\{[K_8(Me_2pz)_8(thf)_2]\cdot\text{THF}\}_\infty$ (**8**) were also isolated from the reaction mixture with the identity determined by X-ray crystallographic analysis.

$[Ce_2(Me_2pz)_6(OtBu)_4K_2]_\infty$ (9):

$[Ce(Me_2pz)_3(thf)]_2$ (0.27 g, 0.27 mmol) and $K(OtBu)$ (0.061 g, 0.54 mmol) were stirred with heating (~60 °C) in PhMe (5 ml) for two days **in a greaseless Schlenk flask**. The resulting light-yellow powder was not entirely soluble in PhMe, and subsequently THF (~1 mL) was added. After several days of stirring, the reaction mixture was evaporated to dryness (in vacuo), and crystallisation from hexane produced small colourless crystals that were not suitable for analysis by X-ray crystallography. Consequently, the crystals were re-dissolved in fresh PhMe (~2 ml) and THF (~2 ml) and heated at (~60 °C) for several days. Addition of hexane and extended heating produced small orange crystals along the Schlenk flask wall. The orange crystals were analysed by X-ray crystallography giving the composition: $[Ce_2(Me_2pz)_6(OtBu)_4K_2]_\infty$ (**9**). Yield = ~0.05 g (15%). Elemental analysis calcd. (%) for $C_{46}H_{78}Ce_2K_2N_{12}O_4$ (1221.62): C 45.23, H 6.44, N 13.76; found: C 45.15, H 6.36, N 13.82.

Acknowledgements

PCJ and GBD gratefully acknowledge the ARC for funding (DP230100112). Parts of this research were undertaken on the MX1 beamline at the Australian Synchrotron, part of ANSTO.[30] We thank Mr. Stephen Boch, Institut für Anorganische Chemie, Universitaet Tübingen for assistance with some microanalyses. Open Access publishing facilitated by James Cook University, as part of the Wiley - James Cook University agreement via the Council of Australian University Librarians.

Conflict of Interests

There are no conflicts of interest to declare.

Data Availability Statement

The data that support the findings of this study are available from the corresponding author upon reasonable request.

Keywords: Lanthanoids · lanthanum · cerium · lithium · potassium · 3,5-dimthylpyrazolate · oxide centred cages · structures

[1] a) H. Schumann, P. R. Lee, J. Loebel, *Angew. Chem., Int. Ed. Engl.* **1989**, *28*, 1033–1035; b) H. Schumann, J. Loebel, J. Pickardt, *Organometallics* **1991**, *10*, 215–219.
[2] M. A. Halcrow, *Dalton Trans.* **2009**, 2059–2073.
[3] C. C. Quitmann, V. Bezugly, F. R. Wagner, K. Müller-Buschbaum, *Z. Anorg, Allg. Chem.* **2006**, *632*, 1173–1186.
[4] J. E. Cosgriff, G. B. Deacon, B. M. Gatehouse, H. Hemling, H. Schumann, *Angew. Chem., Int. Ed. Engl.* **1993**, *32*, 874–875.
[5] J. E. Cosgriff, G. B. Deacon, B. M. Gatehouse, H. Hemling, H. Schumann, *Aust. J. Chem.* **1994**, *47*, 1223–1235.
[6] J. E. Cosgriff, G. B. Deacon, B. M. Gatehouse, *Aust. J. Chem.* **1993**, *46*, 1881–1896.
[7] G. B. Deacon, B. M. Gatehouse, S. Nickel, S. N. Platts, *Aust. J. Chem.* **1991**, *44*, 613–621.
[8] J. E. Cosgriff, G. B. Deacon, B. M. Gatehouse, P. R. Lee, H. Schumann, Z. Anorg, *Allgem. Chem.* **1996**, *622*, 1399–1403.
[9] G. B. Deacon, R. Harika, P. C. Junk, B. W. Skelton, D. Werner, A. H. White, *Eur. J. Inorg. Chem.* **2014**, 2412–2419.
[10] D. Werner, U. Bayer, N. E. Rad, P. C. Junk, G. B. Deacon, R. Anwander, *Dalton Trans.* **2018**, *47*, 5952–5955.
[11] D. Werner, G. B. Deacon, P. C. Junk, R. Anwander, *Dalton Trans.* **2017**, *46*, 6265–6277.
[12] D. Werner, G. B. Deacon, P. C. Junk, R. Anwander, *Eur. J. Inorg. Chem.* **2017**, 3419–3428.
[13] U. Bayer, D. Werner, C. Maichle-Mössmer, R. Anwander, *Angew. Chem., Int. Ed. Engl.* **2020**, *59*, 5830–5836.
[14] D. Werner, N. E. Rad, Z. Guo, G. B. Deacon, P. C. Junk, Z. Anorg, *Allg. Chem.* **2022**, *648*(1–7), e202200222.
[15] X. Zhou, Z. Huang, R. Cai, L. Zhang, L. Zhang, *Organometallics* **1999**, *18*, 4128–4133.
[16] S. De, A. Mondal, S. R. Giblin, R. A. Layfield, *Angew. Chem. Int. Ed.* **2024**, *63*, e202317678.
[17] a) J. A. Cotruvo, *ACS Cent. Sci.* **2019**, *5*, 1496–1506; b) O. A. Mironova, A. A. Ryadun, T. S. Sukhikh, N. A. Pushkarevsky, S. N. Konchenko, *New J. Chem.* **2023**, *47*, 3406–3416.
[18] D. B. G. Williams, M. Lawton, *J. Org, Chem.* **2010**, *75*, 8351–8354.
[19] D. R. Burfield, K.-H. Lee, R. H. Smithers, *J. Org, Chem.* **1997**, *42*, 3060–3065.
[20] a) R. E. Mulvey, V. L. Blair, W. Clegg, A. R. Kennedy, J. Klett, L. Russo, *Nat. Chem.* **2010**, *2*, 588–591; b) R. E. Mulvey, *Dalton Trans.* **2013**, *42*, 6676–6693; c) C. Pan, S. Sheng, J. Wang, Y. Pan, *Mendeleev Commun.* **2011**, *21*, 318–319.
[21] G. B. Deacon, E. E. Delbridge, D. J. Evans, R. Harika, P. C. Junk, B. W. Skelton, A. H. White, *Chem. Eur. J.* **2004**, *10*, 1193–1204.
[22] G. B. Deacon, A. Gitlits, P. W. Roesky, M. K. Bürgstein, K. C. Lim, B. W. Skelton, A. H. White, *Chem. Eur. J.* **2001**, *7*, 127–138.
[23] G. A. Bowmaker, Effendy, P. J. Harvey, P. C. Healy, B. W. Skelton, A. H. White, *J. Chem. Soc., Dalton Trans.* **1996**, 2459–2465.
[24] Z. Guo, N. Wang, V. L. Blair, E. I. Izgorodina, G. B. Deacon, P. C. Junk, *Aust. J. Chem.* **2022**, *75*, 558–565.
[25] S. Alvarez, *Dalton Trans.* **2013**, *42*, 8617–8636.
[26] S. S. Batsanov, *Inorg. Mater.* **2001**, *37*, 871–885.
[27] M.-A. Velazquez-Carmona, A.-J. Metta-Magana, S.-A. Cortes-Llamas, V. Montiel-Palma, M.-A. Munoz-Hernandez, *Polyhedron* **2009**, *28*, 205–208.
[28] S.-Á. Cortés-Llamas, R. Hernández-Lamoneda, M.-Á. Velázquez-Carmona, M.-A. Muñoz-Hernández, R. A. Toscano, *Inorg. Chem.* **2005**, *45*, 286–294.
[29] S.-Á. Cortés-Llamas, M.-Á. Velázquez-Carmona, M.-Á. Muñoz-Hernández, *Inorg. Chem. Commun.* **2005**, *8*, 155–158.
[30] N. P. Cowieson, D. Aragao, M. Clift, D. J. Ericsson, C. Gee, S. J. Harrop, N. Mudie, S. Panjikar, J. R. Price, A. Riboldi-Tunnicliffe, R. Williamson, T. Caradoc-Davies, *J. Synchrotron Rad.* **2015**, *22*, 187–190.

Manuscript received: August 8, 2024
Revised manuscript received: September 24, 2024
Accepted manuscript online: October 16, 2024
Version of record online: November 14, 2024